Evolution of copper resistance in the kiwifruit pathogen *Pseudomonas syringae* pv. *actinidiae* through acquisition of integrative conjugative elements and plasmids

Elena Colombi[1], Christina Straub[1], Sven Künzel[2], Matthew D. Templeton[3,4], Honour C. McCann[1,5*], Paul B. Rainey[1,2,6*]

[1]New Zealand Institute for Advanced Study, Massey University, Auckland, New Zealand. [2]Max Planck Institute for Evolutionary Biology, Plön, Germany. [3]Plant and Food Research, Auckland, New Zealand. [4]School of Biological Sciences, University of Auckland, Auckland, New Zealand. [5]South China Botanical Institute, Chinese Academy of Sciences, Guangzhou, China. [6]Ecole Supérieure de Physique et de Chimie Industrielles de la Ville de Paris (ESPCI Paris-Tech), PSL Research University, Paris, France. * Joint senior authors

Correspondence: Elena Colombi, New Zealand Institute for Advanced Study, Massey University, Private Bag 102 904, Auckland 0745, New Zealand. Telephone: +64 9 4140800 ext 43810. e-mail: e.colombi@massey.ac.nz

Running title: Evolution of copper resistance

ORIGINALITY-SIGNIFICANT STATEMENT

Lateral gene transfer is a major evolutionary force, but its immediacy is often overlooked. Between 2008 and 2010 a single virulent clone of the kiwifruit pathogen *Pseudomonas syringae* pv. *actinidiae* spread to kiwifruit growing

regions of the world. After arrival in New Zealand it acquired genetic determinants of copper resistance in the form of integrative conjugative elements and plasmids. Components of these elements are evident in distantly related bacteria from millet (USA, 1921), kiwifruit (Japan, 1988) and wheat (New Zealand, 1968). Additional laboratory experiments capture evidence of the dynamism underpinning the evolution of these elements in real time and further emphasize the potent role that lateral gene transfer plays in microbial evolution.

SUMMARY

Lateral gene transfer can precipitate rapid evolutionary change. In 2010 the global pandemic of kiwifruit canker disease caused by *Pseudomonas syringae* pv. *actinidiae* (*Psa*) reached New Zealand. At the time of introduction, the single clone responsible for the outbreak was sensitive to copper, however, analysis of a sample of isolates taken in 2015 and 2016 showed that a quarter were copper resistant. Genome sequences of seven strains showed that copper resistance – comprising *czc*/*cusABC* and *copABCD* systems – along with resistance to arsenic and cadmium, was acquired via uptake of integrative conjugative elements (ICEs), but also plasmids. Comparative analysis showed ICEs to have a mosaic structure, with one being a tripartite arrangement of two different ICEs and a plasmid that were isolated in 1921 (USA), 1968 (NZ) and 1988 (Japan), from *P. syringae* pathogens of millet, wheat and kiwifruit, respectively. Two of the *Psa* ICEs were nearly identical to two ICEs isolated from kiwifruit leaf colonists prior to the introduction of *Psa* into NZ. Additionally, we show ICE transfer *in vitro* and *in planta*, analyze fitness consequences of ICE carriage, capture the *de novo* formation of novel recombinant ICEs, and explore ICE host-range.

INTRODUCTION

Horizontal gene transfer (HGT) is a potent evolutionary process that significantly shapes patterns of diversity in bacterial populations. Horizontally transmissible elements, including plasmids, phages and integrative conjugative elements (ICEs) move genes over broad phylogenetic distances and mediate abrupt changes in niche preferences (Sullivan and Ronson, 1998; Ochman *et al*., 2000; Ochman *et al.*, 2005; Guglielmini *et al*., 2011).

ICEs are plasmid-like entities with attributes of temperate phages that disseminate vertically as part of the bacterial chromosome and horizontally by virtue of endogenously encoded machinery for conjugative transfer (Wozniak and Waldor, 2010; Guglielmini *et al*., 2011). Essential genetic modules include those mediating integration, excision, conjugation and regulation of conjugative activity (Mohd-Zain *et al*., 2004; Juhas *et al*., 2007; Roberts and Mullany, 2009). During the process of conjugation ICEs circularize and transfer to new hosts, leaving a copy in the original host genome (Wozniak and Waldor, 2010; Johnson and Grossman, 2015). Conjugation during pathogenesis is often regulated by environmental signals (Lovell *et al*., 2009; Quiroz *et al*., 2011; Vanga *et al*., 2015).

In addition to a set of essential genes, ICEs often harbour "cargo" genes of adaptive significance to their hosts. These include genes affecting biofilm formation, pathogenicity, antibiotic and heavy metal resistance, symbiosis and bacteriocin synthesis (Peters *et al*., 1991; Rauch *et al*., 1992; Ravatn *et al*., 1998; Beaber *et al*., 2002; Drenkard *et al*., 2002; Burrus *et al*., 2006; Ramsay *et al*., 2006; Dimopoulou *et al*., 2007; Kung *et al*., 2010). The genetic information stored in cargo genes varies considerably causing ICEs to range in size from 20 kb to

500 kb (Johnson and Grossman, 2015).

In 2008 a distinct and particularly virulent form of the kiwifruit pathogen *Pseudomonas syringae* pv. *actinidiae* (*Psa*) was identified in Italy. It was subsequently disseminated throughout kiwifruit growing regions of the world causing a global pandemic that reached New Zealand (NZ) in 2010 (Balestra *et al*., 2010; Abelleira *et al*., 2011; Everett *et al*., 2011; Vanneste *et al*., 2011). Genomic analysis showed that although the pandemic was derived from a single clone it acquired a set of distinctive ICEs during the course of its global journey (Mazzaglia *et al*., 2012; Butler *et al*., 2013; McCann *et al*., 2013). The NZ lineage carries Psa_{NZ13}ICE_eno which harbours a 20 kb "enolase" region that is also found in otherwise divergent *Psa* ICEs (McCann *et al*., 2013; McCann *et al.*, 2016).

Copper sprays have long been used in NZ to protect plants from a range of diseases. Since the arrival *Psa* in NZ kiwifruit orchardists have employed copper based products to protect vines. From 2011 an ongoing industry-based programme has been in place to monitor copper resistance. In 2014 evidence was first obtained of *Psa* isolates resistant to copper sulphate. Given that the clone of *Psa* originally introduced into NZ was sensitive to copper and lacked genes encoding copper resistance (McCann *et al*., 2013), detection of copper resistance raised the possibility that the evolution of copper resistance in *Psa* is an evolutionary response to the use of copper-based sprays.

Here we report the phenotypic and genetic basis of copper resistance in NZ isolates of *Psa* and show that its emergence has been fuelled by lateral gene transfer involving ICEs and plasmids. We additionally describe the mosaic structure of ICEs, show the dynamics of ICE transfer both *in vitro* and *in planta*,

analyze fitness consequences of ICE carriage, capture the *de novo* formation of novel recombinant ICEs, and explore ICE host-range.

RESULTS

Occurrence of copper resistance in *Psa*

Psa NZ13, isolated in 2010 and representative of the clone introduced in New Zealand, lacks genes encoding copper resistance (McCann *et al*., 2013) and is unable to grow at copper concentrations in excess of 0.8 mM $CuSO_4$. Prior to 2014 no copper resistant or tolerant strains had been reported. However, in 2014, two strains isolated from two different kiwifruit orchards, *Psa* NZ45 and *Psa* NZ47, displayed copper resistance, with a MIC of 1.2 mM $CuSO_4$. This finding prompted a small-scale sampling of both copper treated and untreated orchards in 2015/2016 encompassing the area where resistance was first identified. From a sample of 213 strains isolated from seven orchards 59 were found to be copper resistant. Copper resistant isolates were sampled from both copper treated and untreated orchards. Additional copper resistant strains were procured from other kiwifruit-growing regions of New Zealand (Figure S1).

ICE and plasmid-mediated acquisition of copper resistance in *Psa*

The genome of the focal copper resistant isolate, *Psa* NZ45, is a direct clonal descendant of the isolate originally introduced into NZ (*Psa* NZ13) (McCann *et al*., 2016), but differs in two significant regards. Firstly, the "native" ICE (Psa_{NZ13}ICE_eno) at *att*-1 (immediately upstream of *clpB*), is located at the second *att* site (*att*-2) immediately downstream of *queC* (Figure 1). Secondly, the

genome harbours a new 107 kb ICE (*Psa*$_{NZ45}$ICE_Cu) integrated at the *att*-1 site: *Psa*$_{NZ45}$ICE_Cu carries genes encoding copper resistance (Figures 1 and 2A).

The genomes of six additional copper resistant *Psa* isolates were also sequenced (Table 1) and as with *Psa* NZ45, reads were aligned against the *Psa* NZ13 reference genome (McCann *et al*., 2013; Templeton *et al.,* 2015). All six harbour mobile elements carrying genes encoding copper resistance. The diversity of these elements and genomic location is shown in Figure 1 and their structure is represented in Figure 2A. All isolates are direct clonal descendants of *Psa* NZ13 and thus share an almost identical genome with the exception of the determinants of copper resistance. In *Psa* NZ47 the genes encoding copper resistance are located on a 90 kb ICE (*Psa*$_{NZ47}$ICE_Cu) integrated at the *att-1* site: the native *Psa*$_{NZ13}$ICE_eno is located at the *att-2* site. *Psa* NZ62 carries an ICE identical to that found in *Psa*$_{NZ47}$ICE_Cu (*Psa*$_{NZ62}$ICE_Cu), but is integrated at the *att-2* site; the native ICE (*Psa*$_{NZ13}$ICE_eno) is absent leaving the *att-1* site unoccupied. Isolate *Psa* NZ63 carries *Psa*$_{NZ45}$ICE_Cu integrated at the *att-1* site, but as in *Psa* NZ62, the native *Psa*$_{NZ13}$ICE_eno has been lost. Copper resistance genes in isolate *Psa* NZ64 are also ICE-encoded, but the NZ64 ICE (*Psa*$_{NZ64}$ICE_Cu) is genetically distinct from both *Psa*$_{NZ47}$ICE_Cu and *Psa*$_{NZ45}$ICE_Cu – at 130 kb, it is also the largest. In NZ64, *Psa*$_{NZ64}$ICE_Cu is located at the *att-1* site and the *att-2* site contains the native (*Psa*$_{NZ13}$ICE_eno) ICE. Isolates *Psa* NZ65 and NZ66 both harbour copper resistance genes on a near identical, 120 kb previously undescribed plasmid (pPsaNZ65 and pPsaNZ66, respectively). The only significant difference among the plasmids is the location of a strepomycin resistance-encoding transposon (see below): both isolates have the original *Psa*$_{NZ13}$ICE_eno integrated at the *att-2* site (Figure 1). *Psa* harbouring

149 copper reistance-encoding ICEs have a MIC $CuSO_4$ of 1.2 mM while the MIC of
150 plasmid-carrying *Psa* 1.5 mM (Table 1).
151 That such a small sample of isolates is each unique with regard to the
152 copper resistance-encoding element points to highly dynamic processes shaping
153 their evolution. Such dynamism has been previously noted among enolase-
154 encoding ICEs obtained from a global collection of epidemic *Psa* isolates
155 (McCann *et al*., 2013) and has been observed elsewhere (Burrus *et al*., 2006,
156 Wozniak and Waldorf, 2010). In this study our samples came from a relatively
157 small geographical location. Two ICEs, *Psa*$_{NZ64}$ICE_Cu and *Psa*$_{NZ47}$ICE_Cu were
158 found in different isolates sampled from the same orchard (one year apart),
159 although the two isolates containing near identical plasmids were isolated from
160 orchards located 100 km apart. Two isolates sampled one year apart from the
161 same location (neighboring orchards in Te Puke) carry the same ICE
162 (*Psa*$_{NZ45}$ICE_Cu=*Psa*$_{NZ63}$ICE_Cu; *Psa*$_{NZ47}$ICE_Cu=*Psa*$_{NZ62}$ICE_Cu) (Table 1).
163 The dynamics of ICE evolution becomes especially evident when placed in
164 the broader context possible by comparisons to ICEs recorded in DNA databases.
165 The core genes of the copper resistance-encoding ICEs from New Zealand *Psa*
166 isolates are syntenous with the core genes of the family of ICEs that includes
167 PPHGI-1 (isolated in 1984 from bean in Ethiopia (Teverson, 1991; Pitman *et al*.,
168 2005) and the three ICEs previously described from *Psa* found in New Zealand
169 (2010), Italy (2008) and China (2010) (McCann *et al*., 2013; Butler *et al*., 2013; E.
170 Colombi, unpublished). *Psa*$_{NZ45}$ICE_Cu is a mosaic of DNA from two known ICEs
171 and a plasmid. It shares regions of near perfect identity (over 66 kb) with ICEs
172 present in the otherwise divergent host genomes of *P. syringae pv. panici* (*Ppa*,
173 LGM2367) isolated from proso millet in Madison (USA) in the 1920s (over the

first 38 kb it differs by just 12 SNPs, and one 144 bp insertion), *P. syringae* pv. *atrofasciens* (*Paf*, ICMP4394) isolated in NZ in 1968 from wheat, and a 70.5 kb plasmid present in a non-pandemic *Psa* strain (J2), isolated in Japan in 1988 (Figure 2B).

Interestingly, two of the ICEs described here have also been found in non-*Psa Pseudomonas* isolated from kiwifruit leaves. *Psa*$_{NZ47}$ICE_Cu shows 99.7% pairwise nucleotide identity with an ICE found in *P. marginalis* ICMP 11289 isolated in 1991 from *A. deliciosa* in Katikati (New Zealand). *Psa*$_{NZ64}$ICE_Cu is almost identical (99.5% nucleotide pairwise identity) to an ICE from *P. syringae* pv. *actinidifoliorum* (*Pfm*) ICMP19497, isolated from kiwifruit in 2010 in Te Puke (New Zealand) (Visnovsky *et al*., 2016) (Table 1). Additionally, a 48 kb segment of coding copper resistance genes *Psa*$_{NZ64}$ICE_Cu shares 99.3% nucleotide pairwise identity with a locus found in *P. azotoformans* strain S4 (Fang *et al*., 2016), which was isolated from soil in 2014 in Lijiang (China). However, the locus from *P. azotoformans* is not associated with an ICE.

Genetic determinants of copper resistance

Copper resistance is typically conferred by operons encoding either copper efflux (*cusABC*) and / or sequestration (*copABCD*) systems, both of which can be under the regulation of the *copRS* / *cusRS* two-component regulatory system (Bondarczuk and Piotrowska-Seget, 2013). ICEs identified in *Psa* isolates harbour operons encoding examples of both resistance mechanisms (and regulators), plus genetic determinants of resistance to other metal ions. In each instance the resistance genes are located within "variable regions" (VR) of ICEs into which cargo genes preferentially integrate (Figure 2A). Delineation of these

variable regions comes from detailed analysis of 32 unique ICEs from the *Pph* 1302A and *Psa* families that will be published elsewhere (E. Colombi, unpublished). Overall there are notable similarities and differences in the organization of the variable regions.

As shown in Figure 2B, the first 38 kb of *Psa*$_{NZ45}$ICE_Cu is almost identical (99.7% identical at the nucleotide level) to *Ppa*$_{LGM2367}$ICE. This region spans the core genes, but extends ~8.2 kb into the variable cargo genes with just two SNPs distinguishing the two ICEs (across the 8.2 kb variable region). Encoded within this region is an integrase, arsenic resistance genes (*arsRBCH*), a gene implicated in cadmium and cobalt resistance (*czcD*) and the *copRS* regulatory system. Partway through *copS* the two ICEs diverge at a recombination breakpoint with the downstream variable region from *Psa*$_{NZ45}$ICE_Cu being homologous to a set of copper resistance genes found on plasmid pPaCu1 from the divergent (non-pandemic) Japanese isolate of *Psa* (J2) (Nakajima *et al*., 2002). This region comprises a putative copper transporting ATPase encoded by *copG* (Gutiérrez-Barranquero *et al*., 2013), *cusABC* genes involved in the detoxification of monovalent cations, including copper and silver (Mergeay *et al*., 2003; Rensing and Grass, 2003) and *copABCD* (Figure 2B). The last 4 kb of the variable region of *Psa*$_{NZ45}$ICE_Cu shares almost complete identity with *Ppa*$_{LGM2367}$ICE (Figure 2B).

Detail of the diversity of copper resistance (and related metal resistance) genes is shown in Figure 3. All elements (ICEs and plasmids) harbour the *copRS* regulatory system and, with the exception of *Psa*$_{NZ47}$ICE_Cu, all carry both *cusABC* and *copABCD*, although their organization varies. For example, while *copABCD* is typical, in *Psa*$_{NZ64}$ICE_Cu *copAB* and *copCD* are organized as two separate operons (Figure 3). The putative copper ABC transport system encoded by *copG*

is a common feature, and determinants of arsenic resistance are present in both *Psa*$_{NZ45}$ICE_Cu and *Psa*$_{NZ64}$ICE_Cu. The putative cadmium and related metal resistance gene, *czcD* is also present on these two ICEs. As noted above, a transposon carrying determinants of streptomycin resistance (*strAB*) is present on plasmids pPsaNZ65 and pPsaNZ66. The transposon is of the Tn*3* family and the cassette bears identity to streptomycin resistance carrying transposons found in *P. syringae* pv. *syringae* B728a (Feil *et al*., 2005), but also on plasmid pMRVIM0713 from *Pseudomonas aeruginosa* strain MRSN17623 (GenBank: KP975076.1), plasmid pPMK1-C from *Klebsiella pneumoniae* strain PMK1 (Stoesser *et al*., 2014), and plasmid pTi carried by *Agrobacterium tumefaciens* LBA4213 (Ach5) (GenBank: CP007228.1).

At the level of the operons determining copper resistance there is marked genetic diversity, however, with the exception of CopR, there is relatively little evidence of within operon recombination. The CusABC system is carried on pPsaNZ65 and pPsaNZ66 (but these are identical) and the ICEs *Psa*$_{NZ45}$ICE_Cu and *Psa*$_{NZ64}$ICE_Cu: CusA, CusB and CusC show 75.8%, 50.0% and 44.8% pairwise amino acid identity, respectively; phylogenetic trees based on protein sequences show congruence (Figure S2). The CopABCD system is present on *Psa*$_{NZ45}$ICE_Cu, *Psa*$_{NZ47}$ICE_Cu, *Psa*$_{NZ64}$ICE_Cu (but CopAB and CopCD are in different locations (Figure 3)) and plasmid pPsaNZ65 (and pPsaNZ66): CopA, CopB, CopC and CopD show 76.4%, 63.1%, 79.1% and 60.8% pairwise amino acid identity, respectively. With the exception of CopC (where bootstrap support is low) phylogenetic trees for each protein show the same overall arrangement (Figure S3). The two component regulatory system *copRS* is also present on each of the elements with the amino acid sequences of CopR showing 84.3% and those of

CopS 63.0% pairwise amino acid identity. Phylogenetic trees show CopS from *Psa*$_{NZ64}$ICE_Cu to be the most divergent, and those from *Psa*$_{NZ45}$ICE_Cu and *Psa*$_{NZ47}$ICE_Cu being most similar: CopR shows the same phylogenetic arrangement, however, CopR sequences from *Psa*$_{NZ45}$ICE_Cu and *Psa*$_{NZ47}$ICE_Cu are identical at the protein level suggesting a recent recombination event (Figure S4).

Psa$_{NZ45}$ICE_Cu imposes no detectable fitness cost and confers a selective advantage _in vitro_ in the presence of copper

To determine whether ICE carriage confers a fitness cost, we took advantage of the fact that *Psa* NZ13 and *Psa* NZ45 are essentially isogenic, with the exception of the additional ICE in *Psa* NZ45 (*Psa*$_{NZ45}$ICE_Cu). Each strain was grown alone and density of cells monitored over a 72 hour period with samples taken every 24 hours. In the absence of copper sulphate, no difference in cell density was detected; however, in the presence of 0.5 and 0.8 mM $CuSO_4$ the density of *Psa* NZ13 was reduced (Figure 4A). There is thus no apparent fitness cost associated with carriage of *Psa*$_{NZ45}$ICE_Cu in the absence of copper sulphate, but there is a fitness advantage in copper-containing environments.

Although carriage of *Psa*$_{NZ45}$ICE_Cu appeared not to affect the growth of *Psa* NZ45 in the absence of copper, a more precise measure of fitness was sought by performing competition experiments in which *Psa* NZ13 and *Psa* NZ45 were co-cultured. For this experiment *Psa* NZ13 was marked with a kanamycin resistance cassette so that it could be distinguished from kanamycin sensitive, copper resistant *Psa* NZ45. Over a 24 hour period where the two strains (founded at equal density) competed for the same resources (in shaken MGY

medium without copper sulphate), the fitness of *Psa* NZ45 was not significantly different to *Psa* NZ13 (1.07 ± 0.04; mean and SEM from 3 independent experiments, each comprised of 3 replicates), indicating no significant detectable cost of carriage of *Psa*$_{NZ45}$ICE_Cu.

Given that the mechanism of copper resistance in *Psa* NZ45 – based upon *copABCD* – likely involves sequestration of copper ions we considered the possibility that this isolate might confer cross protection to non-copper resistant isolates, such as *Psa* NZ13. To this end we performed co-culture experiments at sub-inhibitory and inhibitory copper sulphate concentrations. Growth of *Psa* NZ13 at sub-inhibitory concentrations of copper sulphate was significantly impaired by the presence of *Psa* NZ45 and this was especially evident at 48 and 72 hours (Figure S5). At the inhibitory copper sulphate concentration, *Psa* NZ13 appeared to benefit from the presence of *Psa* NZ45. Again, this was most evident at 48 and 72 hours (Figure S5).

Psa$_{NZ45}$ICE_Cu imposes no detectable fitness cost and confers no selective advantage _in planta_

Cost and benefit of carrying *Psa*$_{NZ45}$ICE_Cu was also evaluated during endophytic colonization of kiwifruit leaves. No significant difference was observed in growth of singly-inoculated *Psa* NZ13 and NZ45 (dip inoculation was used to found colonization). Spray application of a commonly used commercial copper-based treatment (Nordox75 (0.375 g L^{-1})) subsequent to dip inoculation resulted in a reduction of bacterial density of both strains and the presence of *Psa*$_{NZ45}$ICE_Cu in *Psa* NZ45 did not confer any advantage *in planta* (Figure 4B). Co-cultivation competition assays in the presence or absence of Nordox75

299 confirmed carriage of *Psa*$_{NZ45}$ICE_Cu imposes no significant fitness cost or
300 advantage during endophytic growth: fitness of NZ45 relative to NZ13 was 1.00
301 ± 0.02 and 1.07 ± 0.03 at day 3 and 7, respectively; fitness of NZ45 relative to
302 NZ13 in the presence of 0.375 g L^{-1} Nordox was 1.15 ± 0.04 and 0.97 ± 0.09 at
303 day 3 and 7, respectively (data are means and SEM from 3 independent
304 experiments, each comprised of 5 replicates; significance was calculated by one
305 sample *t*-test).
306
307 **_Psa_$_{NZ45}$ICE_Cu transfer dynamics _in vitro_ and _in planta_**
308 Acquisition of *Psa*$_{NZ45}$ICE_Cu (and related ICEs) by *Psa* NZ13 suggests that
309 the element is active and capable of self-transmission. If so, then it is possible
310 that transfer may have occurred during the course of the co-cultivation
311 experiments used to determine cost of ICE carriage. To determine whether this
312 had happened samples from the mixtures were plated on MGY medium
313 containing both kanamycin and copper sulphate. Copper resistant, kanamycin
314 resistant transconjugants were detected both *in vitro* and *in planta.* This means
315 that a fraction of *Psa* NZ13 strains acquired *Psa*$_{NZ45}$ICE_Cu. These
316 transconjugants marginally inflate the counts of *Psa* NZ45, however, the number
317 of transconjugants (see below) was several orders of magnitude less that *Psa*
318 NZ13, thus having no appreciable effect on the measures of relative fitness.
319 At 24 hours in shaken MGY broth transconjugants were present at a
320 frequency of 5.04 ± 2.25 x 10^{-3} per recipient cell (mean and SEM from 3
321 independent experiments, each comprised of 3 replicates). Analysis of samples
322 from *in planta* experiments showed that at 3 days, transconjugants were present
323 at a frequency of 2.05 ± 0.63 x 10^{-2} per recipient cell (mean and SEM from 3

independent experiments, each comprised of 5 replicates). On plants in the presence of Nordox (0. 375 g L^{-1}) the frequency of transconjugants was 9.37 ± 1.56 x 10^{-2} per recipient three days after inoculation (mean and SEM from 3 independent experiments, each comprised of 5 replicates). Transfer was also observed in M9 agar, on M9 agar supplemented with 0.5mM $CuSO_4$, on M9 agar supplemented with a macerate of Hort16A fruit with transconjugants present (at 48 hours) at a frequency of 2.16 ± 0.9 x 10^{-5}, 1.11 ± 0.4 x 10^{-5} and 1.98 ± 0.8 x 10^{-5} per recipient cell, respectively.

To explore the dynamics of transfer *in vitro*, samples from shaken MGY cultures were taken hourly, for six hours, and then at 24 hours. The data, presented in Figure 5, show acquisition of *Psa*$_{NZ45}$ICE_Cu by *Psa* NZ13 within one hour of the mating mix being established (approximately 1 recipient per 10^5 recipient cells). The frequency was relatively invariant over the subsequent six hour period, but rose to approximately 1 recipient in 10^3 cells at 24 hours.

Detection of ICE transfer just one hour after mixing donor and recipient cells promoted a further experiment in which transconjugants were assayed at 10 minute intervals. From three independent experiments, each with five replicates, transconjugants were detected at 30 mins (approximately 4 x 10^{-7} transconjugants per recipient cell).

Analysis of co-cultivation experiments from kiwifruit leaves showed evidence that *Psa*$_{NZ45}$ICE_Cu also transferred *in planta.* The frequency of transconjugants at day 3 and day 7 was approximately 1 per 50 recipient cells and the frequency of transconjugants was not affected by changes in the initial founding ratios of donor and recipient cells (Table S1). Overall, the frequency of

transconjugants was approximately three orders of magnitude greater *in planta* than *in vitro*.

ICE displacement and recombination

To check the genetic composition of transconjugants and to investigate whether *Psa*$_{NZ45}$ICE_Cu integration in recipient cells occurred at the *att-1* or *att-2* site, a set of primers were designed to identify the location of ICE integration in the *Psa* NZ13 genome (Table S2). 11 independently generated transconjugants from shaken MGY culture were screened. As expected, successful amplification of primers annealing to *copABCD* in *Psa*$_{NZ45}$ICE_Cu was observed in all transconjugants, while amplification of the *enolase* gene primers (indicative of the presence of the native *Psa*$_{NZ13}$ICE_eno) occurred only in *Psa* NZ13 and *Psa* NZ45 (Figure S6). However, in two transconjugants only the *IntPsaNZ13-att-1* primer pair resulted in amplification, suggesting that recombination between *Psa*$_{NZ45}$ICE_Cu and *Psa*$_{NZ13}$ICE_eno had occurred (Figure S7). Genome sequencing of one of these transconjugants revealed a recombination event inside the variable region of the ICE that produced a chimeric ICE identical to *Psa*$_{NZ45}$ICE_Cu up to and including the CuR operon, with the remainder identical to the downstream segment of *Psa*$_{NZ13}$ICE_eno (Figure 6).

Psa$_{NZ45}$ICE_Cu can be transferred to a range of *P. syringae* strains

The host range of the *Psa*$_{NZ45}$ICE_Cu was characterised using a panel of nine different *Pseudomonas* strains as recipients, representing the diversity of *P. syringae* and the genus more broadly. Transfer of *Psa*$_{NZ45}$ICE_Cu to *Psa* J31, *Pfm* NZ9 and *P. syringae* pv. *phaseolicola* (*Pph*) 1448a (on M9 agar plates) was

observed with the frequency of transconjugants per recipient cell being 7.64 ± 1.7 x 10^{-6}, 7.74. ± 2.5 x 10^{-7} and 1.23 ± 0.2 x 10^{-4}, respectively. No transconjugants were detected for *P. aeruginosa* PAO1, *P. fluorescens* SBW25, *P. syringae* pv. *tomato* DC3000 or *Psa* K28, despite the fact that these three strains have both *att* sites.

DISCUSSION

The importance and impact of lateral gene transfer on the evolution of microbial populations has long been recognized (Sullivan *et al*., 1995; Lilley and Bailey, 1997; Ochman *et al*., 2000; Ochman *et al*., 2005; Wozniak and Waldor, 2010; Polz *et al*., 2013). Here we have captured the real time evolution of copper resistance in a plant pathogen, in an agricultural setting, and shown that movement of copper resistance genes occurs primarily via ICEs. The strains subject to genomic analysis provide a glimpse of just how dynamic evolution fuelled by ICEs can be. Of the seven copper resistant *Psa* isolates analyzed, five contain copper resistance-encoding ICEs – three unique ICEs in total – with variable placement within the *Psa* genome, including movement and instability of the native ICE (Psa_{NZ13}ICE_eno). Further evidence of dynamism comes from *in vitro* and *in planta* studies, which show not only transfer to isogenic *Psa* and unrelated *P. syringae* strains, but also the ready formation of chimeras between Psa_{NZ45}ICE_Cu and Psa_{NZ13}ICE_eno. Mosaicism of ICEs has been reported elsewhere and is often promoted by the presence of tandem copies (Garriss *et al*., 2009; Wozniak and Waldor, 2010). The ease with which ICEs move between strains and capacity for intra-ICE recombination emphasizes the futility of drawing conclusions on strain phylogeny based on ICE phylogeny (McCann *et al*.,

398 2013), but also the impossibility of understanding ICE evolution based on the
399 phylogeny of ICEs themselves.
400 Evidence of the formation of chimeric ICEs extends beyond the ICEs
401 studied here. *Psa*$_{NZ45}$ICE_Cu is a recombinant of two previously reported ICEs
402 and a plasmid: most surprising is the fact that the recombinant components are
403 derived from elements isolated from three geographic regions (USA, Japan and
404 New Zealand) from three different plants (millet, kiwifruit and wheat) and
405 spanning almost 100 years. Additionally, two of the copper resistance-encoding
406 ICEs found in *Psa* (*Psa*$_{NZ47}$ICE_Cu and *Psa*$_{NZ64}$ICE_Cu) have been reported in other
407 kiwifruit leaf colonizing organisms emphasizing the ease by which self-
408 transmissible elements can move between members of a single community.
409 Clearly the potency of evolution fuelled by ICEs with the *P. syringae* complex is
410 remarkable, with impacts likely extending well beyond that inferred from the
411 analysis of genome sequences (Fondi *et al*., 2016).
412 Evidence of the spectrum and dynamic of transfer inferred from the
413 genomic analysis of natural isolates is bolstered by demonstration of the *in vitro*
414 and *in planta* transfer of *Psa*$_{NZ45}$ICE_Cu. The fact that *Psa*$_{NZ45}$ICE_Cu can be
415 detected in a recipient strain just 30 minutes after mixing with a donor strain (in
416 shaken broth culture) points to an as yet undetermined proficiency for transfer
417 and possible regulatory mechanism. At the same time, the frequency of
418 transconjugants *in planta* are several orders of magnitude greater than *in vitro*
419 suggesting even greater potential (perhaps regulated) for transfer in the natural
420 environment.
421 The selective causes underpinning the evolution of copper resistance in
422 *Psa* is uncertain and to date copper resistance is not known to have evolved

423 outside of New Zealand. While it is tempting to blame use of copper sprays by
424 orchardists, it is possible that the evolution of copper resistant *Psa* is a more
425 general response to copper levels in New Zealand soils combined with long-term
426 use of copper-based sprays in New Zealand agriculture (Morgan and Taylor,
427 2004). Support for this stems from the fact that *Psa*$_{NZ47}$ICE_Cu shows almost
428 perfect identify with an ICE found in *P. marginalis* (ICMP 11289) from kiwifruit
429 isolated in 1991 (in New Zealand). In addition, copper resistance-encoding ICEs
430 were found in both copper treated, and untreated orchards. There is need to
431 understand further the population ecology of copper-resistance ICEs at regional,
432 national and global scales and the selective causes for their maintenance and
433 spread (Staehlin *et al*., 2016).

434 The impact of the copper resistance-encoding ICEs on fitness *in planta* –
435 in the presence of copper sprays – appears to be minimal. While this is
436 heartening news from the perspective of control of the pathogen, there are at
437 least three reasons to treat this result with caution. Firstly, it is difficult to
438 accurately assess fitness *in planta* and it is possible that our measures
439 underestimate the contribution of copper resistance to growth in the presence of
440 copper: even a 1% increase in fitness over 24 hours, which is beyond
441 experimental capacity to detect, can have significant long-term consequences.
442 Secondly, the presence of copper resistance genes means opportunity for levels
443 of resistance to increase through, for example, promoter mutations that increase
444 levels of transcription of resistance determinants, or through acquisition of
445 additional copper resistance-encoding genes. Thirdly, and perhaps most
446 significantly, is the fact that the copper resistance-encoding ICEs confer no
447 measurable fitness cost even in the absence of copper. This suggests that these

448 elements will not be readily lost from *Psa* populations even if copper-based
449 sprays were eliminated (Andersson and Hughes, 2010; Neale *et al.*, 2016). That
450 some strains of the global pandemic now contain two ICEs gives reason to
451 suspect elevated evolutionary potential among these isolates.

452 While the focus of our investigation has been copper resistance, the ICEs
453 reported here carry a cargo of additional genes, some of which are implicated in
454 resistance to other metals. In some instances the cargo genes have no similarity
455 to genes of known function (grey boxes in Figure 2A). ICEs and similar laterally
456 transferred elements provide opportunity for genes unrelated to copper
457 resistance, for example gene connected to virulence, to hitchhike and rapidly
458 spread. In this regard the two plasmids characterized here are of interest: both
459 carry determinants of streptomycin resistance – an antibiotic that is also sprayed
460 on New Zealand kiwifruit orchards in order to control *Psa.* The potential for
461 hitchhiking has been previously noted in the context of antibiotic resistance-
462 encoding plasmids (Gullberg *et al.*, 2014).

463 Recognition of ICEs along with their potential to change the course of
464 microbial evolution extends less than twenty years (Wozniak and Waldor, 2010).
465 While it might be argued that this potential is no different from that long realized
466 via conjugative plasmids, or phage (Ochman *et al.*, 2000), ICEs, being a composite
467 of both, seem to have an edge. Unlike conjugative plasmids that rarely integrate
468 into the host genome, ICEs integrate as a matter of course and are largely
469 immune to segregational loss; additionally, fitness consequences as a result of
470 carriage are likely to be minimal. Unlike temperate phages, ICEs do not kill the
471 host upon transfer, but they can nonetheless mediate transfer upon
472 encountering transfer proficient conditions. Having control over both vertical

and horizontal modes of transmission, while minimizing costs for host cells, marks these elements as especially potent vehicles of microbial evolution.

EXPERIMENTAL PROCEDURES

Strains and culture condition

All *Pseudomonas* strains were cultured in King's B medium at 28˚C, *E. coli* was cultured in Luria Bertani medium at 37˚C. All liquid overnight cultures were shaken at 250 rpm. Both kanamycin and nitrofurantoin were used at 50 μg mL^{-1}.

DNA extraction and genome sequencing

For genome sequencing, DNA samples were extracted using the Promega Wizard® Genomic DNA Purification Kit following the recommended protocol. *Psa* NZ45 was sequenced using the PacBio platform, the remainder were sequenced using the Illumina HiSeq platform. Sequences are deposited at NCBI with the following accession numbers: XXXX1, XXXX2 etc (right number of accession numbers).

Genomic reconstruction of ICEs

ICEs identified in genome sequences were used as query sequences for BLAST searches of the NCBI WGS database (http://blast.ncbi.nlm.nih.gov/Blast.cgi). Contigs were subsequently downloaded and where ICEs were represented by two contigs they were concatenated in Geneious (http://www.geneious.com, Kearse *et al.*, 2012). Concatenation was only required in two instances. ICEs were annotated using

497 the RAST server (http://rast.nmpdr.org, Aziz *et al.*, 2008) and manually curated.
498 Alignments were performed using Geneious.
499
500 **_Psa_ isolation from kiwifruit orchards**
501 One cm^2 kiwifruit leaf disks were macerated in 200 µl 10mM $MgCl_2$. The
502 macerate was plated on *Pseudomonas* selective media amended with cetrimide,
503 fucidin and cephalosporin (Oxoid) and incubated at 28˚C for 3 days. *Psa* was
504 identified using either diagnostic PCR or LAMP assays (Rees-George *et al*., 2010,
505 Ruinelli *et al*., 2016).
506
507 **Copper resistance assays**
508 Copper resistance was evaluated by determining the minimal
509 concentration of copper that inhibited growth (minimal inhibitory
510 concentration, MIC) on mannitol-glutamate yeast extract medium (MGY) plates
511 supplemented with $CuSO_4 \cdot 5H_2O$ (Bender and Cooksey, 1986, Cha and Cooksey
512 1991). *Psa* strains were considered resistant when their MIC exceeded 0.8 mM
513 $CuSO_4$.
514
515 **Mutant development**
516 A Tn*5* transposon was used to generate kanamycin resistant (*kanR*)
517 strains. *E. coli* S17-1 Tn*5hah Sgid1* (Zhang *et al.*, 2015) was used as donor and *E.*
518 *coli* pK2013 (Ditta *et al.,* 1980) as helper. Helper, donor and recipients were
519 grown overnight. 200 µl of helper and donor and 2 mL of recipient were
520 separately washed with 10mM $MgCl_2$ and then mixed together and washed
521 again. The mix was then re-suspended in 30 µl of 10 mM $MgCl_2$, plated on pre-

warmed LB agar plates and incubated for 24-48 hours at 28˚C. Cells were then harvested, resuspended in 1ml of sterile 10 mM $MgCl_2$ and plated on KB kanamycin nitrofurantoin plates. Selected mutants were screened for normal growth in KB, LB and M9.

In vitro growth

Overnight cultures of *Psa* NZ13^{kanR} and *Psa* NZ45 were used to determine the *in vitro* growth of each strain in MGY alone or supplemented with 0.5 and 0.8mM $CuSO_4$. 10mL liquid MGY cultures were established with a starting density of 10^5 cfu mL^{-1} and shaken for up to three days. Bacterial growth was monitored by plating on KB kanamycin (*Psa* NZ13^{kanR}), MGY 0.8mM $CuSO_4$ (*Psa* NZ45). Three replicates per strain and media combination was used, and the experiment was repeated three times.

In planta growth

Clonally propagated *Actinidia chinensis* var. 'Hort16A' plantlets were maintained at 20˚C with a light/dark period of 14/10 hours, 70% constant humidity. *Psa* NZ13^{kanR} and *Psa* NZ45 were grown on KB agar plates for 48h at 28˚C. Inoculum with a final optical density (OD_{600}) of 0.2 of either strain was prepared in 50 ml 10mM $MgCl_2$ with 0.002% of Silwet. Three to four week old plantlets were inoculated by dipping the aerial parts in the inoculum solution for 5 seconds. Five separate plantlets were dip inoculated for each treatment. For experiments assessing *in planta* growth in copper-sprayed plantlets, Nordox75 was used at the recommended dosage of 0.375g L^{-1}. (www.kvh.org.nz/spray_products). Dip-inoculated plantlets were allowed to dry,

547 then sprayed adaxially and abaxially with Nordox75 until runoff to ensure
548 complete coverage. Bacterial growth was monitored 0, 3 and 7 days post
549 inoculation. 1 cm^2 disk leaves were cut using a sterile cork borer, surface
550 sterilized in 70% ethanol and ground in 200 µl 10mM $MgCl_2$. Serial dilutions of
551 the homogenate were plated on KB kanamycin to count *Psa* NZ13^{kanR} and MGY
552 0.8mM $CuSO_4$ to count *Psa* NZ45.Each experiment was repeated 3 times.
553
554 **_In vitro_ and _in planta_ competition assays**
555 *In vitro* and *in planta* competition assays were conducted as described
556 earlier for single strains, except that *Psa* NZ45 and *Psa* NZ13^{kanR} were
557 coinoculated in a 1:1 mix. Bacterial growth was monitored by plating serial
558 dilutions on KB kanamycin (*Psa* NZ13^{kanR}), MGY 0.8mM $CuSO_4$ (*Psa* NZ45) and on
559 MGY kanamycin 0.8mM $CuSO_4$ (*Psa*NZ13^{kanR} that acquired copper resistance). *In*
560 *vitro* assays had three replicates per strain, *in planta* assays were conducted
561 using five replicates, each experiment was repeated three times. Fitness was
562 calculated as ratio between their Malthusian Parameters (Lenski *et* al., 1991).
563
564 **ICE integration screening**
565 Primers used in this study are listed in Supp Table 2. Four primers were
566 designed to detect the genomic location of ICE integration: two specific for the
567 integrases at the end of each ICEs (*IntPsaNZ45*, *IntPsaNZ13*) and two for the ICE
568 insertion site on the chromosome, annealing to the *clpB* (*att-1* site) and *queC*
569 (*att-2* site) genes. The primer combination (*IntPsaNZ45-att-2*, *IntPsaNZ45-att-1*,
570 *IntPsaNZ13-att-1*, and *IntPsaNZ13-att-2*) indicates the location of the ICEs.
571 Another two sets of primers were designed to amplify either CuR (*copA*) or

572 enolase genes present in the VR of *Psa*$_{NZ45}$ICE_Cu and *Psa*$_{NZ13}$ICE_eno,
573 respectively. PCRs were performed using Thermo Scientific *Taq DNA Polymerase*
574 following the manufacturer's instructions.
575
576 **ICE mobilization assay**
577 *Psa* NZ45 was used as the ICE donor. Strains tested in the mobilization
578 assays included are listed in order of divergence relative to the donor: *Psa* K28
579 (biovar 2) (McCann *et al*., 2013), *Psa* J31 (biovar 1) (McCann *et al*., 2013),
580 *Peusomonas syringae* pv. *actinidifoliorum* NZ9 (McCann *et al*., 2013),
581 *Pseudomonas syringae* pv. *tomato* DC3000 (Buell *et al*., 2003), *Pseudomonas*
582 *syringae* pv *phaseolicola* 1448a (Teverson, 1991), *Pseudomonas syringae* H24 and
583 H33 (isolated from kiwifruit; C. Straub, unpublished data), *Pseudomonas*
584 *fluorescens* SBW25 (Zhang *et al*., 2006) and *Pseudomonas aeroginosa* PAO1
585 (Holloway, 1955). The copper sulphate MIC was determined for all tested
586 recipient strains, which were all tagged with kanamycin Tn*5*. A biparental
587 mating was performed using 2 mL and 200µl of washed recipient and *Psa* NZ45
588 cells, respectively. The cells were mixed, centrifuged briefly and resuspended in
589 30µl of 10 mM $MgCl_2$ alone, 10 mM $MgCl_2$ with 0.5mM $CuSO_4$ or 30 µl of 1 cm^2
590 kiwifruit plantlet macerate in 200µl of 10 mM $MgCl_2$ if requested. The cell
591 mixture was plated onto solid media (M9 plates) and incubated at 28˚C for 48
592 hours. Cells were then harvested and resuspended in 1ml of sterile 10 mM $MgCl_2$.
593 Serial dilutions were plated on KB kanamycin to count the total number of
594 recipients and on MGY amended with kanamycin and copper sulphate at
595 recipient MIC to count transconjugants.
596

Biosecurity and approval

All worked was performed in approved facilities and in accord with APP201675, APP201730, APP202231.

ACKNOWLEDGMENTS

We gratefully acknowledge Zespri International Limited and Te Puke Fruit Growers Association for financial support. The sponsors had no role in the design, collation, or interpretation of data. We thank kiwifruit growers in Te Puke for the access to orchards, Denis Robinson for providing Nordox75, and Daniel Rexin for assistance with isolating *Psa* from kiwifruit leaves.

REFERENCES

Abelleira, A., López, M.M., Peñalver, J., Aguín, O., Mansilla, J.P., Picoaga, A. and García, M.J. (2011) First report of bacterial canker of kiwifruit caused by *Pseudomonas syringae* pv. *actinidiae* in Spain. Plant Dis 95: 1583.

Andersson, D.I. and Hughes, D. (2010) Antibiotic resistance and its cost: is it possible to reverse resistance? Nature Reviews Microbiology 8: 260–271.

Aziz, R.K., Bartels, D., Best, A.A., DeJongh, M., Disz, T., Edwards, R.A. *et al*. (2008) The RAST Server: rapid annotations using subsystems technology. BMC Genomics 9: 75-10.1186/1471-2164-9-75.

Balestra, G.M., Renzi, M. and Mazzaglia, A. (2010) First report of bacterial canker of *Actinidia deliciosa* caused by *Pseudomonas syringae* pv. *actinidiae* in Portugal. New Dis Rep 22: 10.

Beaber, J.W., Hochhut, B. and Waldor, M.K. (2002) Genomic and functional analyses of SXT, an integrating antibiotic resistance gene transfer element

622 derived from *Vibrio cholerae*. J Bacteriol 184: 4259–4269.

623 Bender, C.L. and Cooksey, D.A. (1986) Indigenous plasmids in *Pseudomonas*
624 *syringae* pv. *tomato*: conjugative transfer and role in copper resistance. J.
625 Bacteriol 165: 534-541.

626 Bondarczuk, K. and Piotrowska-Seget, Z. (2013) Molecular basis of active copper
627 resistance mechanisms in Gram-negative bacteria. Cell Biol Toxicol 29: 397–
628 405.

629 Buell, C.R., Joardar, V., Lindeberg, M., Selengut, J., Paulsen, I.T., Gwinn, M.L. *et al*.
630 (2003) The complete genome sequence of the Arabidopsis and tomato
631 pathogen *Pseudomonas syringae* pv. *tomato* DC3000. Proc Nat Acad Sci U S A
632 100: 10181–10186.

633 Burrus, V., Marrero, J. and Waldor, M.K. (2006) The current ICE age: biology and
634 evolution of SXT-related integrating conjugative elements. Plasmid 55: 173–
635 183.

636 Butler, M.I., Stockwell, P.A., Black, M.A., Day, R.C., Lamont, I.L. and Poulter, R.T.M.
637 (2013) *Pseudomonas syringae* pv. *actinidiae* from recent outbreaks of kiwifruit
638 bacterial canker belong to different clones that originated in China. PLoS ONE
639 8: e57464.

640 Cha, J.S. and Cooksey, D.A. (1993) Copper hypersensitivity and uptake in
641 *Pseudomonas syringae* containing cloned components of the copper resistance
642 operon. Appl Environ Microbiol 59: 1671–1674.

643 Dimopoulou, I.D., Kartali, S.I., Harding, R.M., Peto, T.E.A. and Crook, D.W. (2007)
644 Diversity of antibiotic resistance integrative and conjugative elements among
645 haemophili. J Med Microbiol 56: 838–846.

646 Ditta, G., Stanfield, S., Corbin, D., Helinski, D.R. (1980) Broad host range DNA

647 cloning system for gram-negative bacteria: construction of a gene bank of
648 *Rhizobium meliloti*. Proc Natl Acad Sci U S A 77: 7347–7351.
649 Drenkard, E. and Ausubel, F.M. (2002) *Pseudomonas* biofilm formation and
650 antibiotic resistance are linked to phenotypic variation. Nature 416: 740–743.
651 Everett, K.R., Taylor, R.K., Romberg, M.K., Rees-George, J., Fullerton, R.A.,
652 Vanneste, J.L. and Manning, M.A. (2011) First report of *Pseudomonas syringae*
653 pv. *actinidiae* causing kiwifruit bacterial canker in New Zealand. Australasian
654 Plant Dis Note 6: 67–71.
655 Fang ,Y., Wu, L., Chen, G., Feng, G. (2016) Complete genome sequence of
656 *Pseudomonas azotoformans* S4, a potential biocontrol bacterium. J Biotechnol
657 227: 25-26.
658 Feil, H., Feil, W.S., Chain, P., Larimer, F., Di Bartolo, G., Copeland, A., *et al.* (2005)
659 Comparison of the complete genome sequences of *Pseudomonas syringae* pv.
660 *syringae* B728a and pv. *tomato* DC3000. Proc Natl Acad Sci U S A 102: 11064-
661 11069.
662 Fondi, M., Karkman, A., Tamminen, M.V., Bosi, E., Virta, M., Fani, R. *et al.* (2016)
663 "Every gene is everywhere but the environment selects": global
664 geolocalization of gene sharing in environmental samples through network
665 analysis. Genome Biol Evol 8: 1388–1400.
666 Garriss, G., Waldor, M.K. and Burrus, V. (2009) Mobile antibiotic resistance
667 encoding elements promote their own diversity. PLoS Genetic 5: e1000775.
668 Guglielmini, J., Quintais, L., Garcillán-Barcia, M. P., de la Cruz, F., Rocha, E.P.
669 (2011) The repertoire of ICE in prokaryotes underscores the unity, diversity,
670 and ubiquity of conjugation. PLoS Genet 7: e1002222.
671 Gullberg, E., Albrecht, L.M., Karlsson, C., Sandegren, L. and Andersson, D.I. (2014)

672 Selection of a multidrug resistance plasmid by sublethal levels of antibiotics
673 and heavy metals. mBio 5: e01918–14.
674 Gutiérrez-Barranquero, J.A., de Vicente, A., Carrión, V.J., Sundin, G.W. and Cazorla,
675 F.M. (2013) Recruitment and rearrangement of three different genetic
676 determinants into a conjugative plasmid increase copper resistance in
677 *Pseudomonas syringae*. Appl Environ Microbiol 79: 1028–1033.
678 Holloway, B.W. (1955) Genetic recombination in *Pseudomonas aeruginosa*. J Gen
679 Microbiol 13: 572–581.
680 Johnson, C.M. and Grossman, A.D. (2015) Integrative and conjugative elements
681 (ICEs): what they do and how they work. Annu Rev Genet 49: 577–601.
682 Juhas, M., Power, P.M., Harding, R.M., Ferguson, D.J., Dimopoulou, I.D., Elamin,
683 A.R., *et al*. (2007) Sequence and functional analyses of *Haemophilus* spp.
684 genomic islands. Genome Biol 8: R237.
685 Kearse, M., Moir, R., Wilson, A., Stones-Havas, S., Cheung, M., Sturrock, S., *et al*.
686 (2012). Geneious Basic: an integrated and extendable desktop software
687 platform for the organization and analysis of sequence data. Bioinformatics
688 28: 1647-1649.
689 Kung, V.L., Ozer, E.A. and Hauser, A.R. (2010) The accessory genome of
690 *Pseudomonas aeruginosa.* Microbiol Mol Biol Rev 74: 621–641.
691 Lenski, R.E., Rose, M.R., Simpson, S.C. and Tadler, S.C. (1991) Long-term
692 experimental evolution *in Escherichia coli*. I. Adaptation and divergence
693 during 2,000 generations. Am Nat 138: 1315–1341.
694 Lilley, A.K., Bailey, M.J. (1997) Impact of plasmid pQBR103 acquisition and
695 carriage on the phytosphere fitness of *Pseudomonas fluorescens* SBW25:
696 burden and benefit. Appl Environ Microbiol 63: 1584–1587.

697 Lovell, H.C., Mansfield, J.W., Godfrey, S.A.C., Jackson, R.W., Hancock, J.T. and
698 Arnold, D.L. (2009). Bacterial evolution by genomic island transfer occurs via
699 DNA transformation *in planta*. Curr Biol 19: 1586–1590.
700 Mazzaglia, A., Studholme, D.J., Taratufolo, M.C., Cai, R., Almeida, N.F., Goodman, T.,
701 *et al*. (2012) *Pseudomonas syringae* pv. *actinidiae* (PSA) isolates from recent
702 bacterial canker of kiwifruit outbreaks belong to the same genetic lineage.
703 PLoS One 7: e36518.
704 Mergeay, M., Monchy, S., Vallaeys, T., Auquier, V., Benotmane, A., Bertin, P., *et al*.
705 (2003) *Ralstonia metallidurans*, a bacterium specifically adapted to toxic
706 metals: towards a catalogue of metal-responsive genes. FEMS Microbiol Rev
707 27: 385–410.
708 McCann, H.C., Rikkerink, E.H.A., Bertels, F., Fiers, M., Lu, A., Rees-George, J., *et al*.
709 (2013) Genomic analysis of the kiwifruit pathogen *Pseudomonas syringae* pv.
710 *actinidiae* provides insight into the origins of an emergent plant disease. PLoS
711 Pathogens 9: e1003503.
712 McCann, H.C., Li, L., Liu, Y., Templeton, M.D., Colombi, E., Straub, C., *et al.* (2016)
713 The origin and evolution of a pandemic lineage of the kiwifruit pathogen
714 *Pseudomonas syringae* pv. *actinidiae*. In review.
715 Mohd-Zain, Z., Turner, S.L., Cerdeno-Tarraga, A.M., Lilley, A.K., Inzana, T.J.,
716 Duncan, A.J., *et al*. (2004) Transferable antibiotic resistance elements in
717 *Haemophilus influenzae* share a common evolutionary origin with a diverse
718 family of syntenic genomic islands. J Bacteriol, 186: 8114–8122.
719 Morgan, R.K. and Taylor, E. (2004) Copper accumulation in vineyard soils in New
720 Zealand. Environ Sci 1:2, 139-167.
721 Nakajima, M., Goto, M. and Hibi, T. (2002) Similarity between copper resistance

722 genes from *Pseudomonas syringae* pv. *actinidiae* and *P. syringae* pv. *tomato*, J
723 Gen Plant Pathol 68: 68–74.
724 Neale, H. C., Laister, R., Payne, J., Preston, G., Jackson, R. W. and Arnold, D. L.
725 (2016) A low frequency persistent reservoir of a genomic island in a pathogen
726 population ensures island survival and improves pathogen fitness in a
727 susceptible host. Environ Microbiol *Accepted Author Manuscript*.
728 doi:10.1111/1462-2920.13482
729 Ochman, H., Lerat, E., Daubin, V. (2005) Examining bacterial species under the
730 specter of gene transfer and exchange. Proc Natl Acad Sci U S A 102 Suppl 1:
731 6595-6599.
732 Ochman, H., Lawrence, J.G. and Groisman, E.A. (2010) Lateral gene transfer and
733 the nature of bacterial innovation. Nature 405: 299–304.
734 Peters, S.E., Hobman, J.L., Strike, P. and Ritchie, D.A. (1991) Novel mercury
735 resistance determinants carried by IncJ plasmids pMERPH and R391. Mol Gen
736 Genet 228: 294–299.
737 Pitman, A.R., Jackson, R.W., Mansfield, J.W., Kaitell, V., Thwaites, R., *et al*. (2005)
738 Exposure to host resistance mechanisms drives evolution of bacterial
739 virulence in plants. Curr Biol 15: 2230–2235.
740 Polz, M.F., Alm, E.J., and Hanage, W.P. (2013) Horizontal gene transfer and the
741 evolution of bacterial and archaeal population structure. Trends Genet 29:
742 170–175.
743 Quiroz, T.S., Nieto, P.A., Tobar, H.E., Salazar-Echegarai, F.J., Lizana, R.J., Quezada
744 C.P., *et al*. (2011) Excision of an unstable pathogenicity island in *Salmonella*
745 *enterica* serovar *enteritidis* is induced during infection of phagocytic cells.
746 PLoS ONE 6: e26031.

747 Ramsay, J.P., Sullivan, J.T., Stuart, G.S., Lamont, I.L. and Ronson, C.W. (2006)
748 Excision and transfer of the *Mesorhizobium loti* R7A symbiosis island requires
749 an integrase IntS, a novel recombination directionality factor RdfS, and a
750 putative relaxase RlxS. Mol Microbiol 62: 723–734.
751 Rauch, P.J.G. and De Vos, W.M. (1992) Characterization of the novel nisin-sucrose
752 conjugative transposonTn5276 and its insertion in *Lactococcus lactis*. J
753 Bacteriol 174: 1280-1287.
754 Ravatn, R., Studer, S., Springael, D., Zehnder, A.J.B. and Van Der Meer, J.R. (1998)
755 Chromosomal integration,tandem amplification, and deamplification in
756 *Pseudomonas putida* F1 of a 105-kilobase genetic element containing the
757 chlorocathecol degradative genes from *Pseudomonas* sp. strain B13. J Bacteriol
758 180: 4360–4369.
759 Rees-George, J., Vanneste, J.L., Cornish, D.A., Pushparajah, I.P.S., Yu, J., Templeton,
760 M.D. and Everett, K.R. (2010) Detection of *Pseudomonas syringae* pv. *actinidiae*
761 using polymerase chain reaction (PCR) primers based on the 16S-23S rDNA
762 intertranscribed spacer region and comparison with PCR primers based on
763 other gene regions. Plant Pathol 59: 453–464.
764 Rensing, C. and Grass, G. (2003) *Escherichia coli* mechanisms of copper
765 homeostasis in a changing environment. FEMS Microbiol Rev 27: 197–213.
766 Roberts, A.P. and Mullany, P. (2009) A modular master on the move: the Tn916
767 family of mobile genetic elements. Trends Microbiol 17: 251–258.
768 Ruinelli, M., Schneeberger, P.H.H., Ferrante, P., Bühlmann, A., Scortichini, M.,
769 Vanneste, J.L., *et al*. (2016) Comparative genomics-informed design of two
770 LAMP assays for detection of the kiwifruit pathogen *Pseudomonas syringae* pv.
771 *actinidiae* and discrimination of isolates belonging to the pandemic biovar 3.

772 Plant Pathol doi:10.1111/ppa.12551.

773 Staehlin, B.M., Gibbons, J.G., Rokas, A., O'Halloran, T.V. and Slot, J.C. (2016)
774 Evolution of a heavy metal homeostasis/resistance island reflects increasing
775 copper stress in *Enterobacteria*. Genome Biol Evol 8: 811-826.

776 Stoesser, N., Giess, A., Batty, E.M., Sheppard, A.E., Walker, A.S., Wilson, D.J., *et al*.
777 (2014) Genome sequencing of an extended series of NDM-producing *Klebsiella*
778 *pneumoniae* isolates from neonatal infections in a Nepali hospital
779 characterizes the extent of community- versus hospital-associated
780 transmission in an endemic setting. Antimicrob Agents Chemother 58: 7347–
781 7357.

782 Sullivan, J.T., Patrick, H.N., Lowther, W.L., Scott, D.B. and Ronson, C.W. (1995)
783 Nodulating strains of *Rhizobium loti* arise through chromosomal symbiotic
784 gene transfer in the environment. Proc Natl Acad Sci USA 92: 8985–8989.

785 Sullivan, J.T. and Ronson, C.W. (1998) Evolution of rhizobia by acquisition of a
786 500-kb symbiosis island that integrates into a phe-tRNA gene. Proc Natl Acad
787 Sci USA 95: 5145–514.

788 Templeton, M.D., Warren, B.A., Andersen, M.T., Rikkerink, E.H.A., Fineran, P.C.
789 (2015) Complete DNA sequence of *Pseudomonas syringae* pv. *actinidiae*, the
790 causal agent of kiwifruit canker disease. Genome Announc 3: e01054-15.

791 Teverson, D.M. (1991) Genetics of pathogenicity and resistance in the halo-blight
792 disease of beans in Africa. Ph.D. thesis. University of Birmingham,
793 Birmingham, United Kingdom.

794 Vanga, B.R., Ramakrishnan, P., Butler, R.C., Toth, I.K., Ronson, C.W., Jacobs, J.M.E.
795 and Pitman, A.R. (2015) Mobilization of horizontally acquired island 2 is
796 induced in plantain the phytopathogen *Pectobacterium atrosepticum*

797 SCRI1043 and involves the putative relaxase ECA0613 and quorum sensing.
798 Environ Microbiol 17: 4730–4744.
799 Vanneste, J.L., Giovanardi, D., Yu, J., Cornish, D.A., Kay, C., Spinelli, F. and Stefani,
800 E. (2011) Detection of *Pseudomonas syringae* pv. *actinidiae* in kiwifruit pollen
801 samples. N Z Plant Protect 64: 246-251.
802 Visnovsky, S.B., Fiers, M., Lu, A., Panda, P., Taylor, R. and Pitman, A.R. (2016)
803 Draft genome sequences of 18 strains of *Pseudomonas* isolated from kiwifruit
804 plants in New Zealand and overseas. Genome Announc 4: e00061–16.
805 Wozniak, R.A.F. and Waldor, M.K. (2010) Integrative and conjugative elements:
806 mosaic mobile genetic elements enabling dynamic lateral gene flow. Nat Rev
807 Microbiol 8: 552–563.
808 Zhang, X.X., Gauntlett, J.C., Oldenburg, D.G., Cook, G.M. and Rainey, P.B. (2015)
809 role of the transporter-like sensor kinase CbrA in histidine uptake and signal
810 transduction. J Bacteriol 197: 2867–2878.
811 Zhang, X.X., George, A., Bailey, M.J. and Rainey, P.B. (2006) The histidine
812 utilization (*hut*) genes of *Pseudomonas fluorescens* SBW25 are active on plant
813 surfaces, but are not required for competitive colonization of sugar beet
814 seedlings. Microbiol 152: 1867–1875.
815

816 **TABLE AND FIGURE**

817

818

819

820

821

822

823

824

825

826

827

828

829

830

831

Isolate ID	Place of Isolation	Year of Isolation	Host of Isolation	Orchard's copper Programme	MIC to $CuSO_4$	GenBank Accession	ICMP number
Psa NZ13	Te Puke, NZ	2010	Kiwifruit	NA	0.8 mM	CP011972.1	18884
Psa NZ45	Te Puke, NZ	2014	Kiwifruit	Full spray	1.2 mM	XXXX1	20586
Psa NZ47	Te Puke, NZ	2014	Kiwifruit	Spray free	1.2 mM	XXXX2	22180
Psa NZ62	Te Puke, NZ	2015	Kiwifruit	Organic	1.2 mM	XXXX3	22181
Psa NZ63	Te Puke, NZ	2015	Kiwifruit	To minimum	1.2 mM	XXXX4	22182
Psa NZ64	Te Puke, NZ	2016	Kiwifruit	Spray free	1.2 mM	XXXX5	22183
Psa NZ65	Te Puke, NZ	2016	Kiwifruit	Full spray	1.5 mM	XXXX6	22184
Psa NZ66	Coromandel, NZ	2016	Kiwifruit	Full spray	1.5 mM	XXXX7	22185
Ppa LGM2367	Madison, USA	1921-1922	Proso millet	NA	NA	ALAC01000019.1; ALAC01000062.1	
Paf ICMP4394	Auckland, NZ	1968	Wheat	NA	NA	LJPO01000111.1; LJPO01000188.1	4394
P. marginalis ICMP4394	Kaikati, NZ	1991	Kiwifruit	NA	NA	LKGX01000080.1	4394
Psa I2	Japan	1988	Kiwifruit	NA	NA	AGNQ01000195	
Pfm ICMP19497	Te Puke, NZ	2010	Kiwifruit	NA	NA	LKBQ01000112.1	19497

832 **Table 1. List of genomes used in this study.**

833

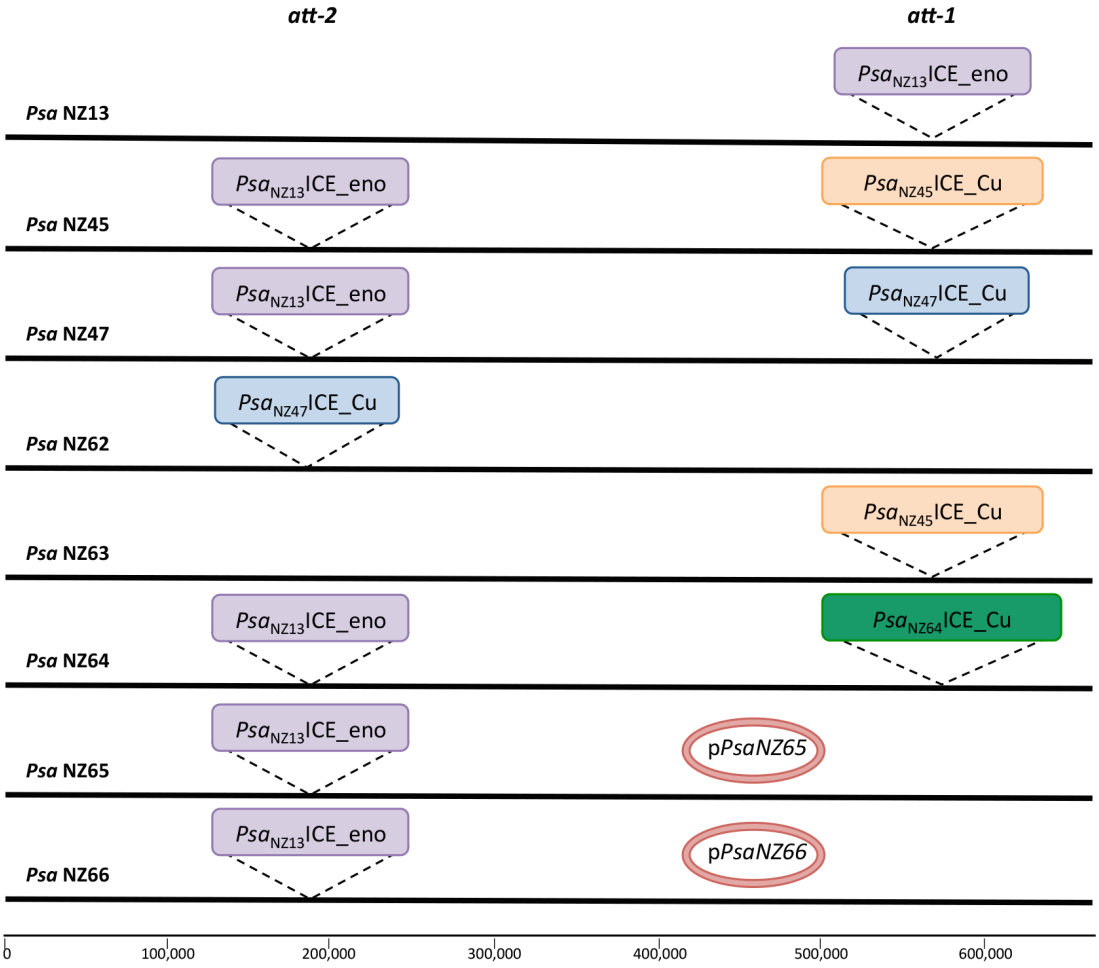

834

835 **Figure 1. Genomic location of *Psa*ICEs in *Psa* NZ13**. In purple the

836 Psa_{NZ13}ICE_eno (100 kb), in orange Psa_{NZ45}ICE_Cu (107 kb), in blue the

837 Psa_{NZ47}ICE_Cu (90 kb), in green the Psa_{NZ64}ICE_Cu (130 kb), pPsaNZ65 and

838 pPsaNZ66 plasmids are 111 kb. Each island is bounded by 52 bp *att* sequences

839 overlapping tRNALys. In *Psa* NZ13 the *att-1* site is located at 5,534,632 bp, *att-2*

840 at 1,733,972 bp. The figure is not to scale (the entire genome of 6.7 Mbp is

841 indicated a single black line). Both Psa_{NZ13}ICE_Eno and Psa_{NZ47}ICE_Cu ICEs were

842 detected in *Psa* NZ47 by sequencing, but analysis of independent colonies from

843 the freezer stock show that Psa_{NZ13}ICE_Eno is prone to loss.

844

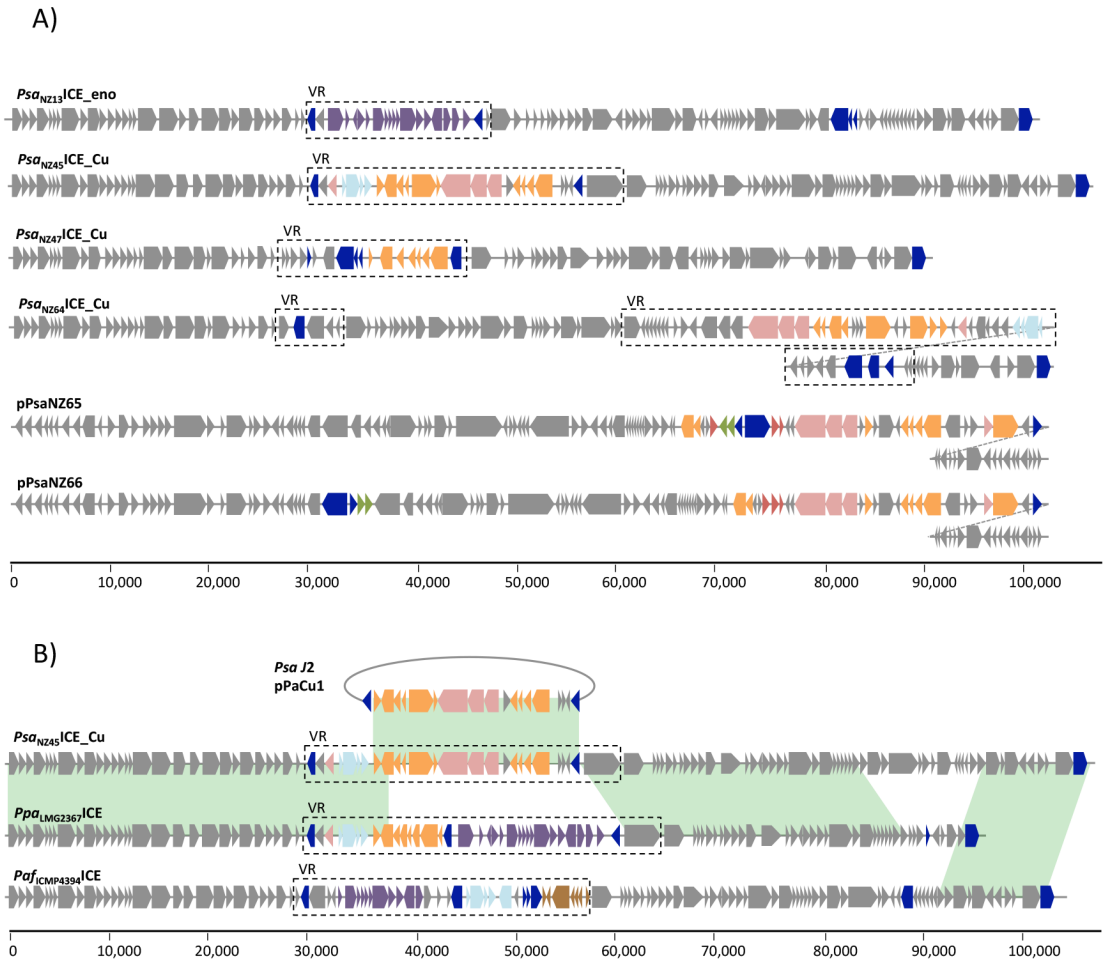

Figure 2. Genetic organization of ICEs and plasmids acquired by *Psa* and mosaicism of *Psa*$_{NZ45}$ICE_Cu.

A) Blue boxes are mobile genes (transposases or recombinases), purple boxes define the 'enolase region', orange boxes depict copper resistance genes, azure boxes are arsenic resistance genes, pink boxes are genes belonging to the *czc*/*cus* system, green boxes are streptomycin resistance genes, red boxes are cation transporter ATPases, brown boxes denote genes encoding mercury resistance. Core "backbone" and other cargo genes are depicted as grey boxes. Dotted diagonal lines indicate continuation of the element.

B) Areas in green show more than 99% pairwise nucelotide identity. *Psa*$_{NZ45}$ICE_Cu and *Ppa*$_{LGM2367}$ICE share identity both in the first 38 kb and 20 kb downstream of VR. The remaining 20 kb of the *Psa*$_{NZ45}$ICE_Cu VR is almost

identical to pPaCu1 (it differs by just 2 SNPs). The last 12.5 kb of *Psa*$_{NZ45}$ICE_Cu is identical to *Paf*$_{ICMP4394}$ICE.

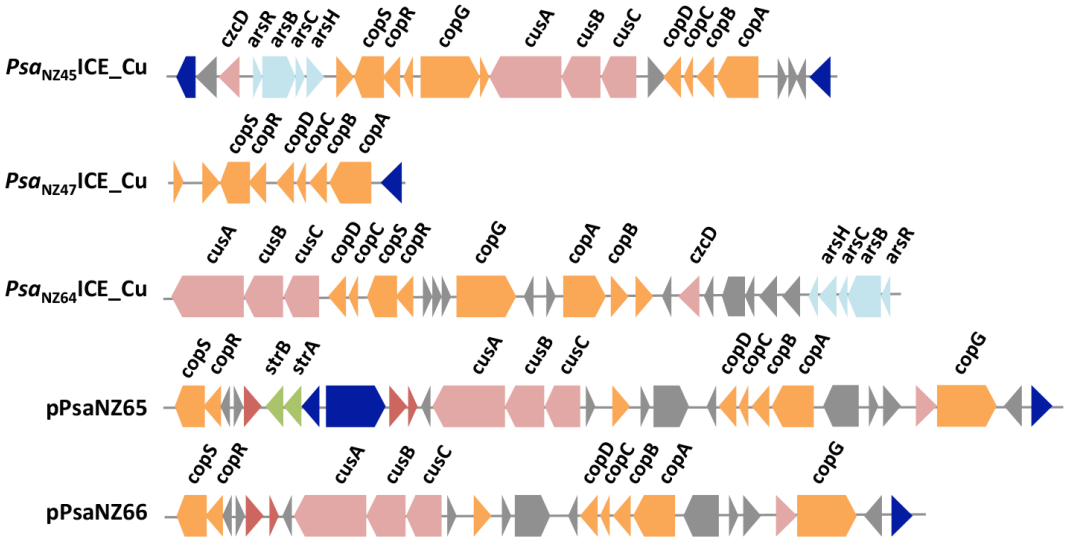

Figure 3. Genetic organization of metal resistance loci. Blue boxes are mobile genes (transposases or recombinases), orange boxes depict copper resistance genes, azure boxes are arsenic resistance genes, pink boxes are genes belonging to the *czc/cus* system, green boxes are streptomycin resistance genes and other genes are depicted as grey boxes.

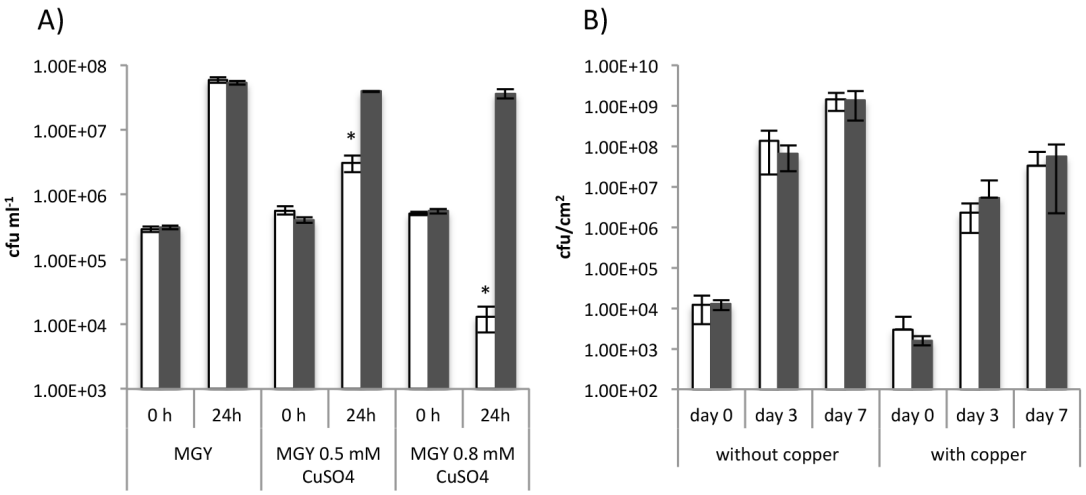

869

870 **Figure 4. Effect of copper ions on growth of *Psa* NZ13 and *Psa* NZ45.**

871 **A)** *Psa* NZ13 (white bars) and *Psa* NZ45 (grey bars) were grown for 24 h in

872 shaken MGY culture and MGY supplemented with 0.5mM and 0.8 mM $CuSO_4$.

873 Data are means and standard deviation of three independent cultures. *indicates

874 significant difference $P<0.05$ (one tailed *t*-test)).

875 **B)** The single growth of *Psa* NZ13 (white bars) and *Psa* NZ45 (grey bars) was

876 assessed endophytically on leaves of the kiwifruit cultivar Hort16A. Data are

877 means and standard deviation of five replicates. The copper product Nordox75

878 (0.375g L^{-1}) was sprayed adaxially and abaxially until run off. Data are means

879 and standard deviation of 5 replicates. One tailed *t*-test showed no statistical

880 difference in growth between of *Psa* NZ13 and NZ45 in absence or presence of

881 copper.

882

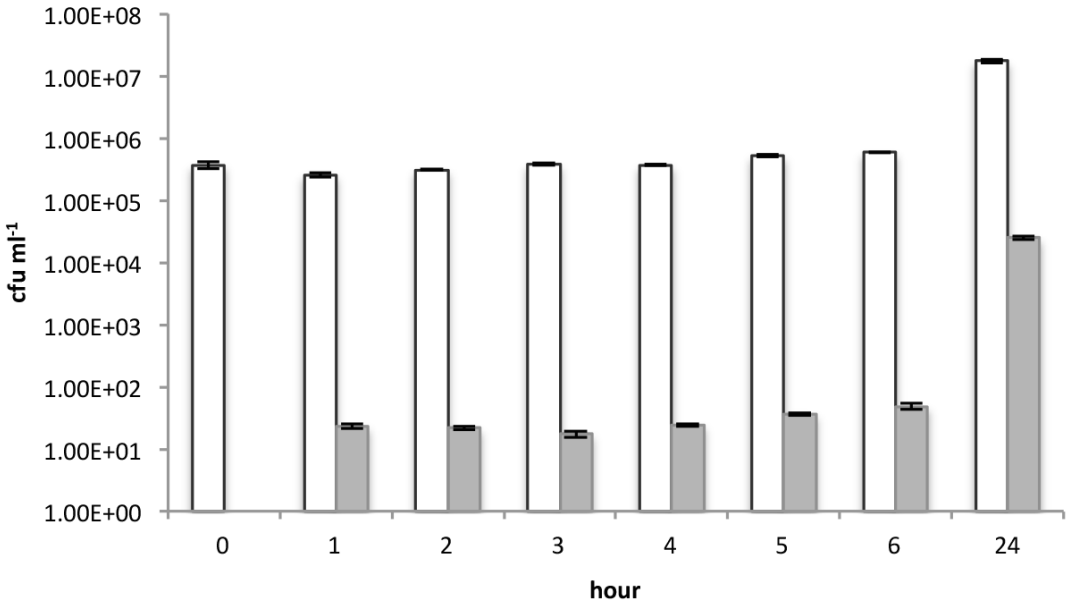

883

884 **Figure 5. *In vitro* transfer of *Psa*$_{NZ45}$ICE_Cu from *Psa* NZ45 to *Psa* NZ13.**

885 Colony forming units of the recipient *Psa* NZ13 (white bars) and *Psa* NZ13

886 carrying *Psa*$_{NZ45}$ICE_Cu (transconjugants, grey bars) was monitored during co-

887 cultivation. Data are means and standard deviation of 3 independent cultures

888

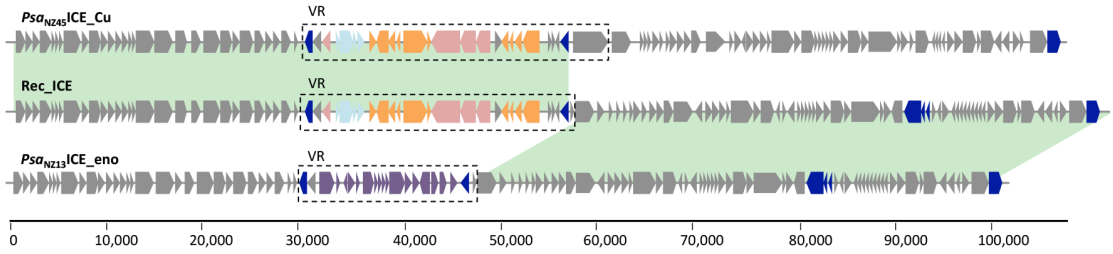

Figure 6. Structure and mosaicism of the recombinant ICE (Rec_ICE) in transconjugant *Psa* NZ13. Areas highlighted in green show 100% pairwise identity. The recombination break point is inside the variable region (VR). Blue boxes are mobile genes (transposases or recombinases), purple boxes define the 'enolase region' (McCann *et al*. 2013), orange boxes depict copper resistance genes, azure boxes are arsenic resistance genes and pink boxes are genes belonging to the *czc*/*cus* system. Core "backbone" and other cargo genes are depicted as grey boxes.

911 **SUPPORTING INFORMATION**

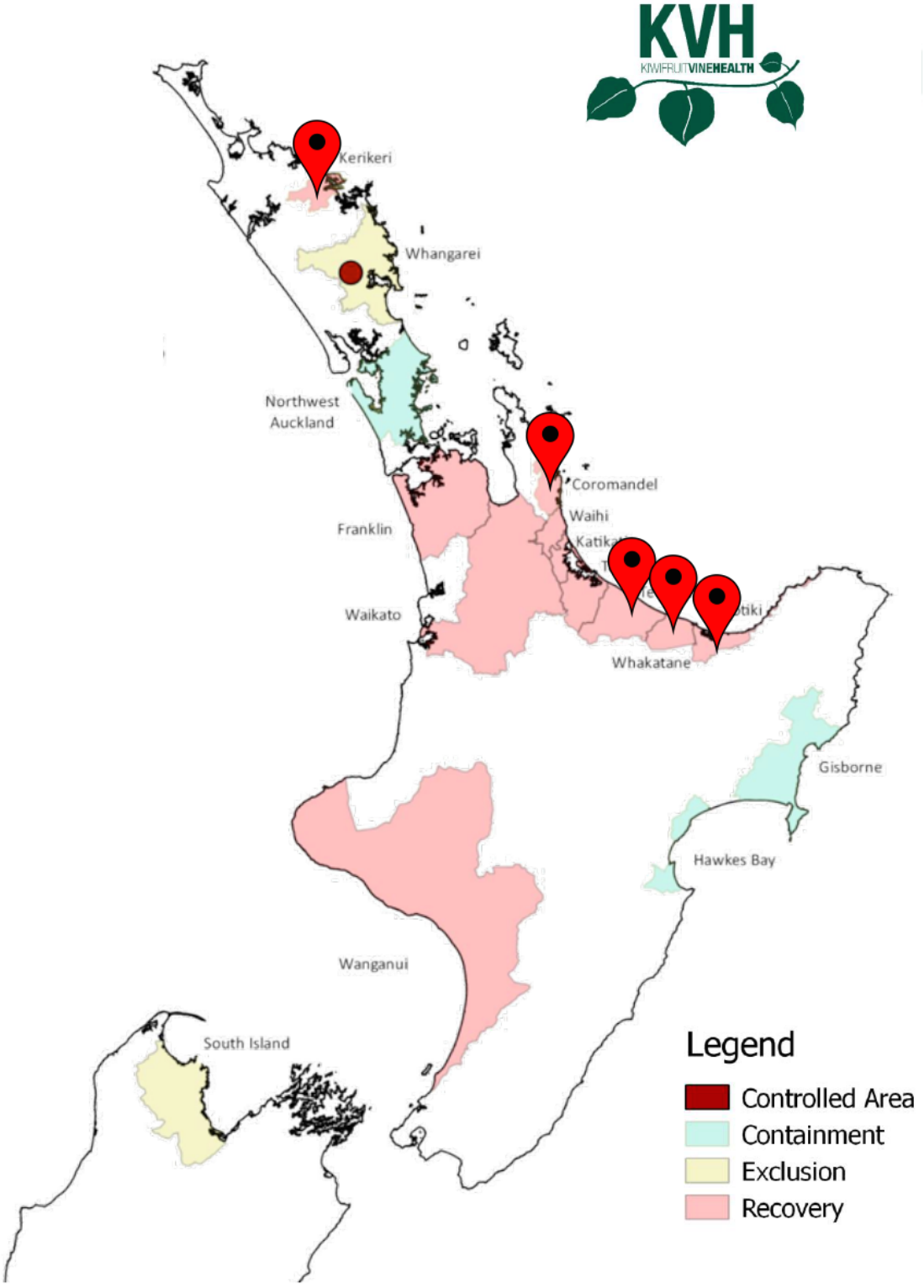

912

913 **Figure S1 –** New Zealand kiwifruit growing regions with isolation sites of copper

914 resistant *Psa.* Map was modified from regional classification map of June 2016

915 (Kiwi Vine Health (KVH)).

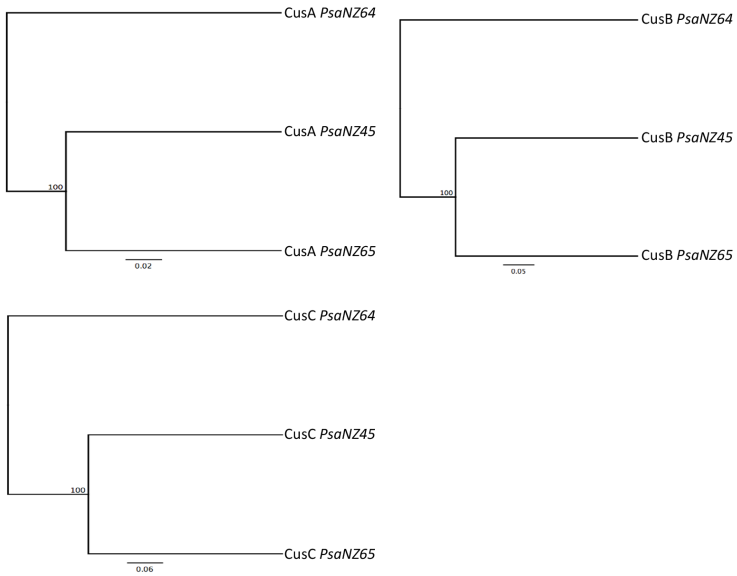

916

917 **Figure S2 – UPMGA tree of the Cus system proteins in *Psa* NZ.** Bootstrap

918 values are shown at each node.

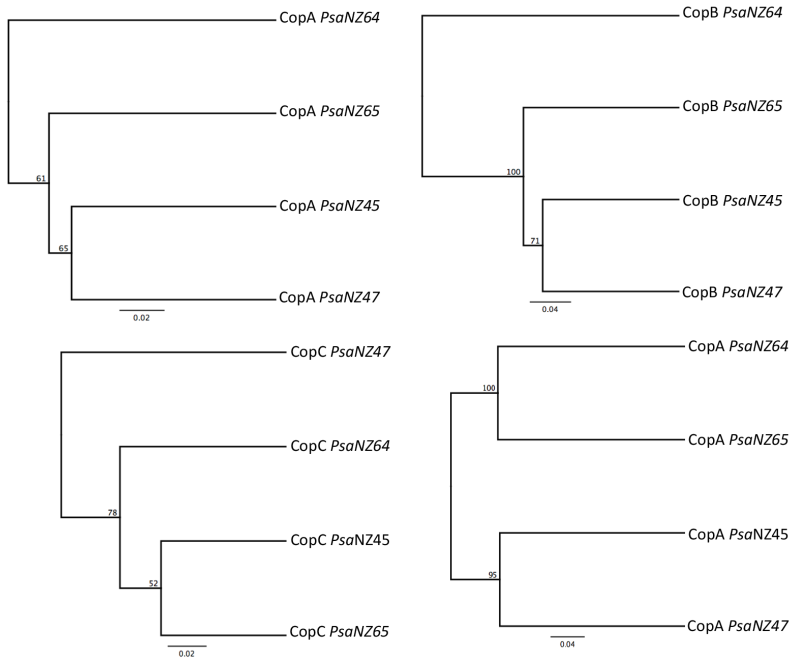

919

920 **Figure S3 – UPMGA trees of the Cop proteins genes in *Psa* NZ.** Bootstrap

921 values are shown at each node.

922

923

924

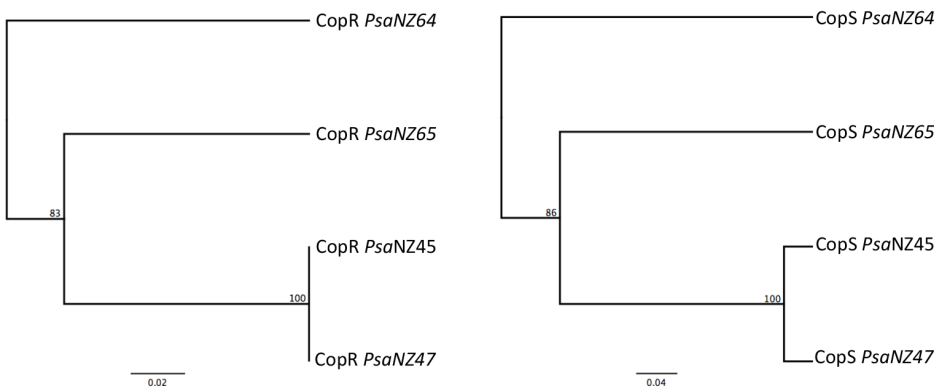

925

926 **Figure S4 – UPMGA trees of CopR and CopS proteins in *Psa* NZ.** Bootstrap

927 values are shown at each node.

928

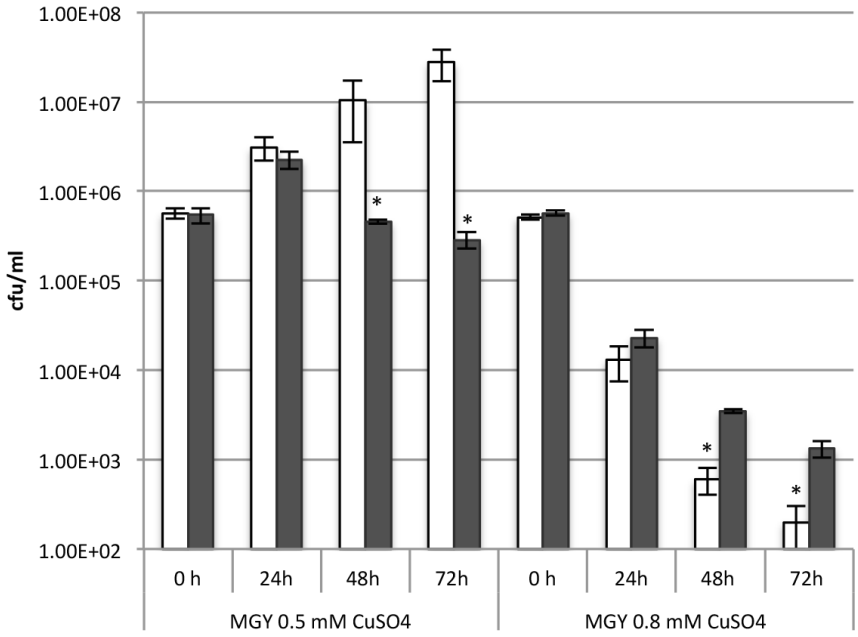

929

930 **Figure S5. Density of single and co-cultured *Psa* in liquid MGY**

931 **supplemented with 0.5 m and 0.8 mM $CuSO_4$.** *Psa* NZ13 was cultured alone

932 (white bars) or co-cultured with *Psa* NZ45 (grey bars). Data are means and

933 standard deviation of three independent cultures. *indicates significance at 5%

934 level by one-tailed *t*-test.

935

936

	Frequency of Psa$_{NZ45}$ICE_Cu transconjugants	
***Psa* NZ13 : *Psa* NZ45**	**day 3**	**day 7**
1 :1	$(2.05 \pm 0.63)^{-2}$	$(2.28 \pm 0.7)^{-2}$
1 : 0.1	$(1.34 \pm 0.52)^{-2}$	$(3.14 \pm 2.3)^{-2}$
0.1 : 1	$(1.68 \pm 0.68)^{-2}$	$(1.88 \pm 0.81)^{-2}$

Table S1. *In planta* transfer of *Psa*$_{NZ45}$ICE_cu from *Psa* NZ45 to *Psa* NZ13 at different founding ratios of donor and recipient. Donor and recipient strains were dip-inoculated onto Hort16A leaves at different founding ratios and frequency of recipients determined at days 3 and 7

Primer name	**Sequence**
copA for	**ATCCGCGGTGACTCGATAAC**
copA rev	**CAGTCGATGGACCGTACTGG**
enolase for	**GAGCTGACGTCCGACATAGAG**
enolase rev	**CCAGTCCAACAGGTTTACCG**
IntPsaNZ13	**GTCAGGCTGATCACTTACGTTG**
IntPsaNZ45	**GTCAGGCTGATCACTAGCGTTA**
att-1	**TGTAGAATAGCGCGCCTCAG**
att-2	**AGCCGTAATCCTGCTGTCC**

Table S2. Primers used for *Psa*$_{NZ13}$ICE_eno and *Psa*$_{NZ45}$ICE_Cu detection and integration loci.

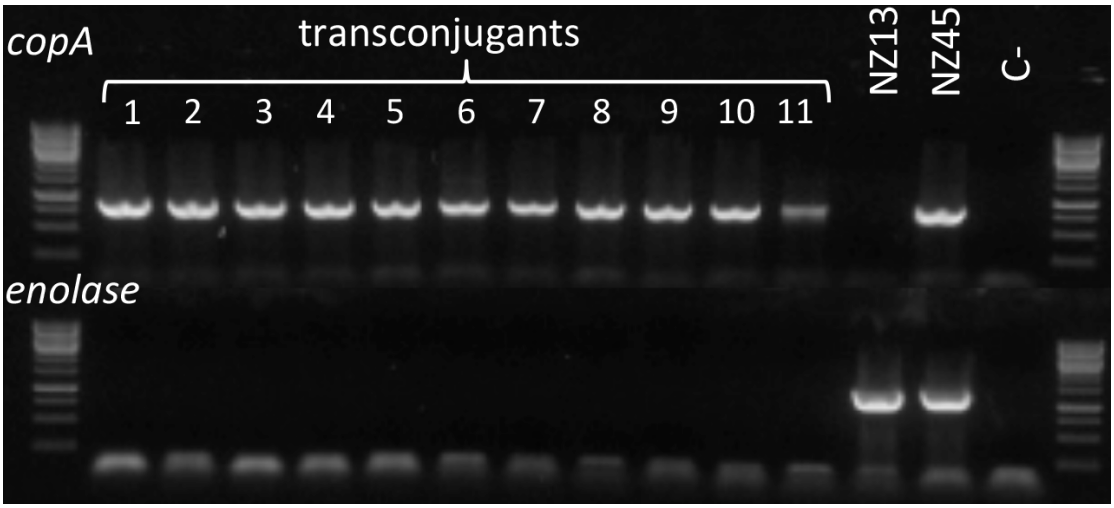

Figure S6. Analysis of the presence of the variable region (VR) of *Psa*$_{NZ45}$ICE_Cu and *Psa*$_{NZ13}$ICE_eno in 11 *Psa* NZ13 transconjugants. PCRs were carried out to detect *copA* (VR of *Psa*$_{NZ45}$ICE_Cu) or *enolase* genes (VR of *Psa*$_{NZ13}$ICE_eno). Controls of *Psa* NZ13 and *Psa* NZ45 show one and two bands, indiciative of *Psa*$_{NZ13}$ICE_eno in *Psa* NZ13 and both *Psa*$_{NZ13}$ICE_eno *Psa*$_{NZ45}$ICE_Cu and in *Psa* NZ45, respectively. All transconjugants, lanes 1-11 have acquired *Psa*$_{NZ45}$ICE_Cu.

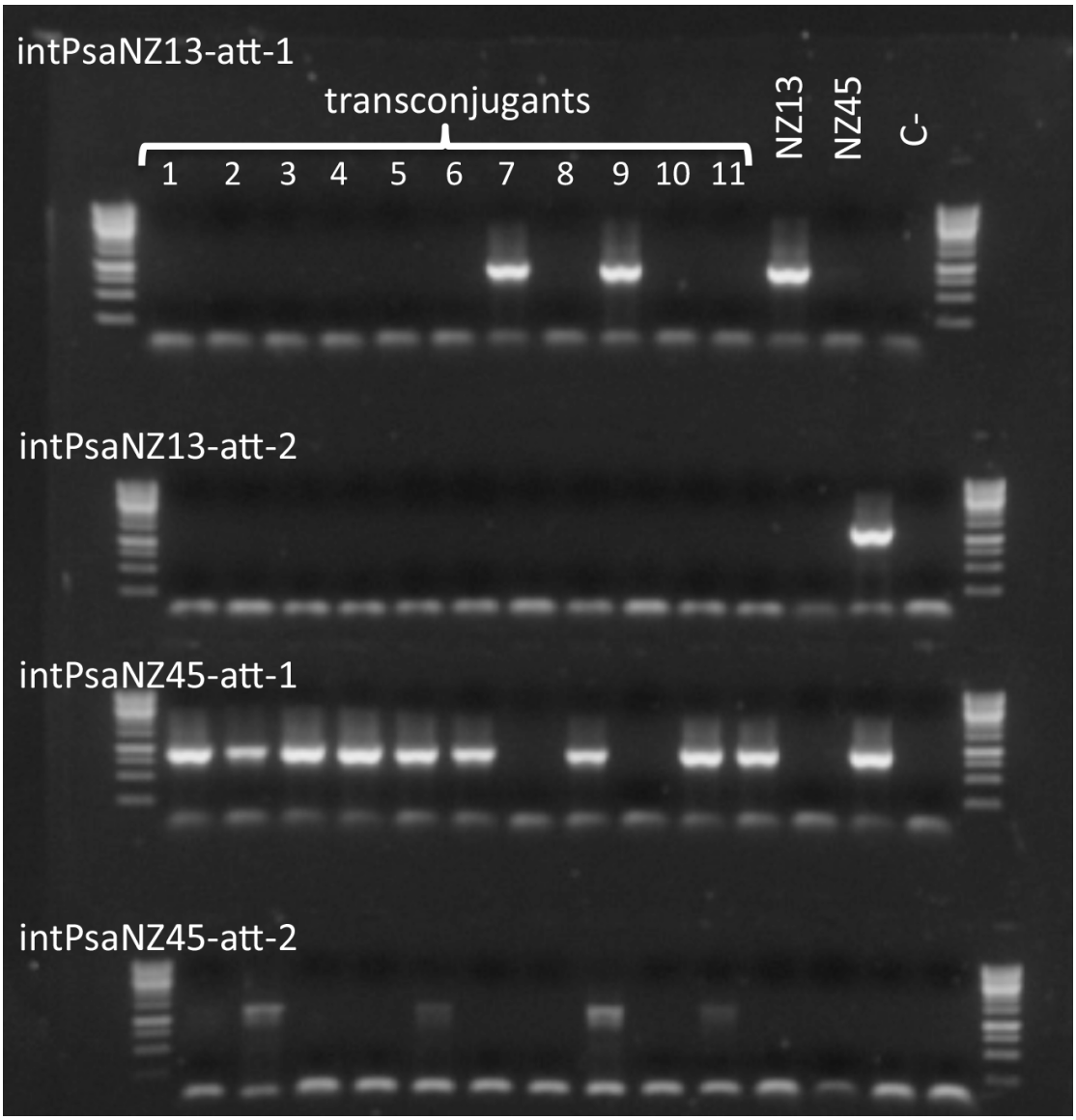

Figure S7. Analysis of the insertion site of the *Psa*$_{NZ13}$ICE_eno and *Psa*$_{NZ45}$ICE_Cu in 11 *Psa* NZ13 transconjugants. PCRs were to detect the integration of *Psa*$_{NZ13}$ICE_eno in the *att-1* or *att-2* sites (*intPsaNZ13-att-1* and *intPsaNZ13-att-2*) and the integration of *Psa*$_{NZ45}$ICE_Cu in the *att-1* or *att-2* sites (*intPsaNZ45-att-1* and *intPsaNZ45-att-2*). Controls of *Psa* NZ13 and *Psa* NZ45 show that in *Psa* NZ13 the *Psa*$_{NZ13}$ICE_eno is integrated in the *att-1* site and in *Psa* NZ45 the *Psa*$_{NZ13}$ICE_eno is integrated in the *att-1* and the *Psa*$_{NZ45}$ICE_Cu in the *att-2* site.